



HAL
open science

Gasification of Low-Grade SRF in Air-Blown Fluidized Bed: Permanent and Inorganic Gases Characterization

Maxime Hervy, Damien Remy, Anthony Dufour, Guillain Mauviel

► **To cite this version:**

Maxime Hervy, Damien Remy, Anthony Dufour, Guillain Mauviel. Gasification of Low-Grade SRF in Air-Blown Fluidized Bed: Permanent and Inorganic Gases Characterization. Waste and Biomass Valorization, 2021, 12 (11), pp.6231-6244. 10.1007/s12649-021-01434-w . hal-03565816

HAL Id: hal-03565816

<https://hal.science/hal-03565816>

Submitted on 17 Feb 2022

HAL is a multi-disciplinary open access archive for the deposit and dissemination of scientific research documents, whether they are published or not. The documents may come from teaching and research institutions in France or abroad, or from public or private research centers.

L'archive ouverte pluridisciplinaire **HAL**, est destinée au dépôt et à la diffusion de documents scientifiques de niveau recherche, publiés ou non, émanant des établissements d'enseignement et de recherche français ou étrangers, des laboratoires publics ou privés.

1 **Gasification of low-grade SRF in air-blown fluidized bed:**
2 **permanent and inorganic gases characterization**

3 Maxime Hervy¹, Damien Remy¹, Anthony Dufour¹, Guillain Mauviel^{1*}

4
5 ¹LRGP, CNRS, Université de Lorraine, ENSIC, 1, Rue Grandville, Nancy, France

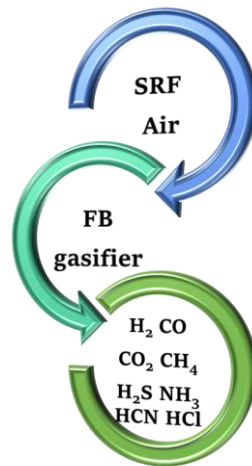
6 Corresponding author: guillain.mauviel@univ-lorraine.fr

7
8 **Abstract**

9 The influence of the gasification temperature and Equivalence Ratio (ER) on the behavior of
10 an industrial low-grade Solid Recovered Fuel (SRF) was investigated in an air bubbling
11 fluidized bed. The studied SRF exhibits an intermediate composition between biomass-rich
12 SRF and plastic-rich SRF. Its Lower Heating Value (14 MJ/kg) is low since its ash content is
13 very high (35 wt.%). But surprisingly, the Cold Gas Efficiency and the Carbon Conversion
14 were relatively high with this type of low-grade SRF. As a result, the syngas produced is quite
15 rich (LHV > 8 MJ/m³ STP) and it may be valorized in gas engines. H₂S, HCl, HCN and NH₃
16 in the syngas were analyzed. These results confirm that inorganic gases are an important issue
17 for the valorization of SRF as fuel in gasification processes, even if significant parts of S, N
18 and Cl are not converted into inorganic gases.

19
20 **Keywords:** SRF; RDF; Gasification; Syngas; Inorganic

23 **Graphical abstract**



24

25 **Statement of Novelty**

26 This work is an original contribution that allows quantifying the different gas species that are
27 obtained through SRF gasification in fluidized bed. These gas species include not only
28 permanent gases, but also inorganic gases like H_2S , NH_3 , HCN , HCl . These data are scarce in
29 the scientific literature, whereas they are required in order to conceive a sustainable gasification
30 process that will produce a purified syngas for CHP applications.

31

32 **Declarations**

33 **Funding:** the research was supported by ADEME through the project ADEME Terracotta n°
34 1606C0013 led by EDF

35 **Conflicts of interest/Competing interests:** No conflict of interest

36 **Availability of data and material:** All the data published in these articles are available for
37 the scientific community

38 **Code availability:** Not applicable

39

40 **1. Introduction**

41 The worldwide production of Municipal Solid Waste (MSW) is estimated around 2.01 billion
42 tons per year, and around 70% of waste is disposed in landfill sites or openly dumped in natural
43 sites [1]. This alarming situation creates catastrophic issues of air, soil, and water pollution
44 affecting human health as well as flora and fauna life [2, 3]. It must prompt the society, starting
45 with the scientific community, to react in order to improve and promote the collection, the
46 recycling and the valorization of wastes [4–10]. While the most efficient solution would consist
47 in the reduction of waste generation, this latter is unfortunately expected to increase to reach
48 3.4 billion tons per year by 2050 [11]. Therefore, new efficient valorization routes must be
49 developed.

50 Solid recovered fuels (SRFs) can be produced by sorting different waste streams and appear as
51 one of the promising solutions to improve waste management [12]. SRFs consist of a mixture
52 of different non-hazardous and non-recyclable solid waste fractions, such as plastics, textiles,
53 tires, paper and carton, biomass waste, or sludge [13]. Consequently, SRFs are very complex
54 and heterogeneous materials, and the proportion of each fraction can vary significantly
55 depending on the waste origin, the season, the waste sorting plant, and the SRF production
56 technique. SRFs represent a significant fuel resource, with a potential estimated at 70 million
57 tons per year in Europe [14]. This resource represents 25-35 Mtep of primary energy, i.e.
58 approximately 2 % of the consumption in Europe [15]. SRFs are complex heterogeneous fuels.
59 Therefore, a rigorous definition of SRF characteristics is difficult to provide, which hinders the
60 development of suitable valorization processes. Currently, SRFs are mainly used as a fuel in
61 cement kiln, but other energetic valorizations are expected to be developed.

62 Thermochemical processes, such as incineration and gasification, are efficient ways for the
63 management of municipal wastes [16, 17], as they allow the decomposition of contaminants

64 and the concentration of some inorganic species in the ashes [18]. In the gasification process,
65 the solid fuel is partially oxidized at high temperature (800-1000 °C) using a gasifying agent
66 (air, steam, O₂ or CO₂). This process results in the production of syngas, composed of a mixture
67 of H₂, CO, CO₂, CH₄, and C_nH_m having high calorific value. One of the most important
68 advantage of gasification over combustion is the different applications existing for the syngas.
69 Depending on its purity, syngas can be used as a fuel in different power generator systems (gas
70 engine, gas turbine, fuel cell), or as a precursor for gaseous fuels (H₂, CH₄) or liquid fuels
71 synthesis [19, 20]. Different gasification technologies have been developed. Among them,
72 fluidized bed reactor is the most adapted for waste valorization at medium-scale (1 to 100
73 MW), due to the efficient flow mixing between reactants, the carefully controlled temperature,
74 the high heat transfer performance, and the large operating flexibility. Indeed, fluidized bed
75 reactor can be operated for the gasification of fuel having different properties [21, 22], such as
76 meat waste and wastewater treatment sludge [23], tires [24, 25], poultry fuel [26], plastic
77 wastes [27–29] etc. For this reason, fluidized bed gasifiers have been used in the past ten years
78 for the gasification of SRFs [30, 31], these materials being very heterogeneous in terms of
79 composition. The LHV of SRF can significantly vary depending on the waste origin and the
80 SRF production method. The valorization of low-grade SRF by gasification process can be
81 impeded if the syngas LHV is too low to be valorized in a gas engine. The presence of
82 pollutants in the syngas (tar, inorganic gases, and particulate matter) also jeopardizes its
83 valorization since it increases the syngas purification cost [32].

84 The pollutants content in syngas strongly depends on the gasification conditions and on the
85 initial fuel composition [33]. For waste gasification, the tar content was proved to be slightly
86 higher than for biomass gasification [30, 34–38]. For this reason, tar removal processes are
87 required before valorizing syngas in gas engines. During waste gasification, the inorganic gases
88 concentration can be significantly higher than that obtained in syngas from biomass due to the

89 high contents in nitrogen, chlorine, and sulphur species initially contained in the waste.
90 Inorganic gases could lead to corrosion and clogging problems in the gasification process, to
91 the poisoning of the catalysts used for syngas cleaning and upgrading, to acid rains [39–41],
92 and also to combustion issue if syngas is burnt in a gas engine [42]. The main inorganic gases
93 contained in syngas are H₂S (100-30000 ppm), HCl (1-500 ppm), NH₃ (500-14000 ppm) and
94 HCN [32, 43–47]. Their content must be drastically reduced to reach the standards required for
95 syngas valorization. For this reason, the measurement of the inorganic gases concentration in
96 syngas from SRF must be accurately carried out.

97 In the literature, different methods have been explored to analyze inorganic gases in syngas.
98 Most of them consists in the absorption of inorganic gases in impingers filled with different
99 solutions which are then analyzed. The composition of the absorbing solutions as well as the
100 analytical tools are different in the studies reported in the literature [31, 48–51]. Indeed, H₂S,
101 NH₃, HCN and HCl after absorption and under ionic state can be analyzed by ion
102 chromatography, potentiometry, iodometry, ion electrophoresis, or indophenols blue
103 absorption spectrophotometry [52]. Syngas can be analyzed on-line (by IR based spectroscopy)
104 but these methods are hardly quantitative due to important artefacts coming from H₂O and CO₂.
105 Sulphur gases can also be directly analyzed by gas chromatography equipped with a PoraPLOT
106 U column and Thermal Conductivity Detector (TCD), but this technique suffers from relatively
107 high detection limit (around 1 ppm) [52, 53] which is typically too high to analyze the syngas
108 purity after the syngas cleaning operations. Pulse Flame Photometer Detector (PFPD) are
109 efficient detectors to analyze inorganic gases, but hydrocarbon species in syngas must be
110 quenched prior to analysis [52]. Recently, new techniques have been developed to analyze S
111 species in syngas of biogas, such as Optical Feedback Cavity-Enhanced Absorption
112 Spectroscopy (OF-CEAS), or ion-molecule reactions-mass spectrometry (IMR-MS) [52].

113 While the decrease in tar concentration with increasing Equivalence Ratio (ER) and
114 gasification temperature was unanimously reported [54, 55], the evolution of inorganic gases
115 with operating conditions in bubbling fluidized bed is currently discussed in the literature.

116 First, concerning the effect of reactor temperature, a temperature rise was proved to increase
117 the release of HCN, while NH₃ decreased [30, 50, 54]. The nature of the solid N-compounds
118 strongly influences the release of nitrogenous species. In carbonaceous materials, different
119 nitrogen groups can be present: pyrrole, pyridine, pyridinium, pyridine oxide, amine, nitro,
120 nitroso, and cyano compounds [56]. NH₃ results from the decomposition of amino-groups,
121 whereas HCN mainly originates from the decomposition of pyrrolic and pyridinic nitrogen
122 [57–60]. As SRFs may be rich in plastics, the gasification performed at relatively high heating
123 rate was proved to promote the release of HCN [61]. While part of the nitrogenous compounds
124 can be in the form of tar [62] and char [63] after pyrolysis, secondary reactions can transform
125 these nitrogenous compounds into HCN during gasification [64]. In addition, the drop of NH₃
126 release with increasing temperature can be attributed to the thermal decomposition of NH₃ into
127 N₂ [65]. This reaction can be catalyzed by the presence of calcium, potassium and iron in the
128 SRF ashes [66]. The HCl content drastically drops with rising temperature [30, 50]. Chlorine
129 in SRF could originate from both organic (PVC) and inorganic (salts) sources [67] which are
130 partially decomposed in the form of HCl during gasification. The decrease of HCl in the gas
131 phase with rising temperature is explained by the presence of alkali metals (especially K).
132 Indeed, at low temperature (<700 °C), alkali species are mainly in the form of alkaline
133 carboxylates. These structures decompose at higher temperature, and alkali metals are then
134 available to react with HCl, which decreases the HCl content in gas phase [68–70]. However,
135 the presence of silica and sulfur in the fuel was proved to increase the HCl formation [67].
136 Sulfur contained in SRF originates from organic and inorganic sources, and elastomers (such
137 as rubber) represent an important input [14]. H₂S is the main S-containing gas released during

138 gasification [47, 71]. A temperature rise was proved to increase the release of H₂S [38, 50, 54].
139 While organic sulfur is decomposed at low temperature (around 500°C) [72], inorganic sulfates
140 in the chars have higher binding energy and are decomposed at higher temperature [73]. Thus,
141 when the temperature increases, higher amount of H₂S is released. Besides, some inorganic
142 species (such as Ca, K or Fe) can react with H₂S to form sulfides and immobilized sulfur in the
143 solid phase, thus decreasing the H₂S release [73, 74]. Nevertheless, *Pinto et al.* observed no
144 effect of temperature on the release of H₂S during the gasification of SRF [31].

145 Second, the influence of the ER on the release of inorganic gases in allothermal gasification
146 reactors is a controversial topic in the literature. The release of inorganic gases could be
147 expected to increase as ER rises, since the secondary reactions (char gasification, tar reforming)
148 could be promoted by oxidation reactions thus favoring the release of Cl, N or S. *Pinto et al.*
149 showed that the ratio of sulphur converted into H₂S to the amount of S in the feedstock
150 increased with increasing ER [31]. It has been reported that the NH₃ concentration increases
151 with rising ER [31, 49]. However, several studies showed that the concentration of inorganic
152 gases (H₂S, HCl, HCN, NH₃) in the syngas decreases with rising ER [50, 54, 75]. This trend
153 can be explained by the promotion of char gasification reactions which promote the contact
154 and reactions between inorganic gases and the mineral species of the ash (Fe, Ca, K, Na)
155 resulting in the immobilization of Cl, N or S atoms in the ashes. This decrease can also be
156 attributed to oxidation reactions promoting the formation of SO_x and NO_x [50]. In addition, the
157 decrease in inorganic gases concentration can result from a dilution effect due to the ER
158 increase. Indeed, when the ER is increased in an air fluidized bed process, the syngas produced
159 is diluted in a larger amount by nitrogen, thus decreasing the inorganic gases concentration.
160 Rigorous measurements must be performed to better understand the distribution of S, Cl, and
161 N.

162 These apparent discrepancies in literature results could be attributed both to the composition
163 of the SRFs studied and to the nature of the bed material. Indeed, the nature of the bed material
164 plays a significant role in the release of inorganic gases. *Pinto et al.* showed that dolomite, lime
165 and olivine allowed to decrease the H₂S content in the syngas [31]. The more reactive materials
166 were dolomite, lime, and finally olivine. This reactivity was attributed to the formation of
167 sulfides by reactions between H₂S and Ca (in dolomite and lime), and to the presence of Fe in
168 olivine. Contradictory results were reported in the literature on the effect of natural minerals
169 on the NH₃ release. Some study highlighted the reduction of NH₃ release with natural minerals
170 [76], while other showed that it increased as these materials catalyzed the char gasification
171 reactions thus promoting the release of heteroatoms [31]. The type of reactor wall, as well as
172 the sampling and analyzing methods were also proved to influence the measurement of
173 inorganic gases [77].

174 Despite all these previous studies, the effect of temperature and ER on the fate of S, Cl, and N
175 species remains unclear.

176 For this reason, the present study investigates the air gasification of an industrial SRF in a
177 fluidized bed. Olivine was used as a common and cheap bed material. At industrial scale, the
178 gasifiers are autothermal, while the reactor walls have to be heated at lab-scale to balance heat
179 losses. Thus, it has been possible to study the respective effects of temperature and ER on the
180 gasification efficiency by varying these two parameters independently. Gasification efficiency
181 was evaluated based on four indicators: cold gas efficiency (CGE), carbon conversion (CC),
182 syngas lower heating value (LHV_{syngas}), and the syngas yield (η_{syngas}). A previous article has
183 presented the effect of gasification conditions on these 4 indicators for two SRFs (one rich in
184 biomass and glass, and a second richer in plastics) [78]. The present article supplements this
185 previous study with another SRF which exhibits an interesting composition between biomass-
186 rich SRF and plastic-rich SRF. Therefore, this SRF presents a complex gasification behavior

187 of high interest for the waste management community. In order to better characterize its
188 gasification behavior, the analysis of the inorganic gases is reported in this study.

189 **2. Materials and methods**

190 **2.1 Characterization of the Solid Recovered Fuel and Fly Ashes**

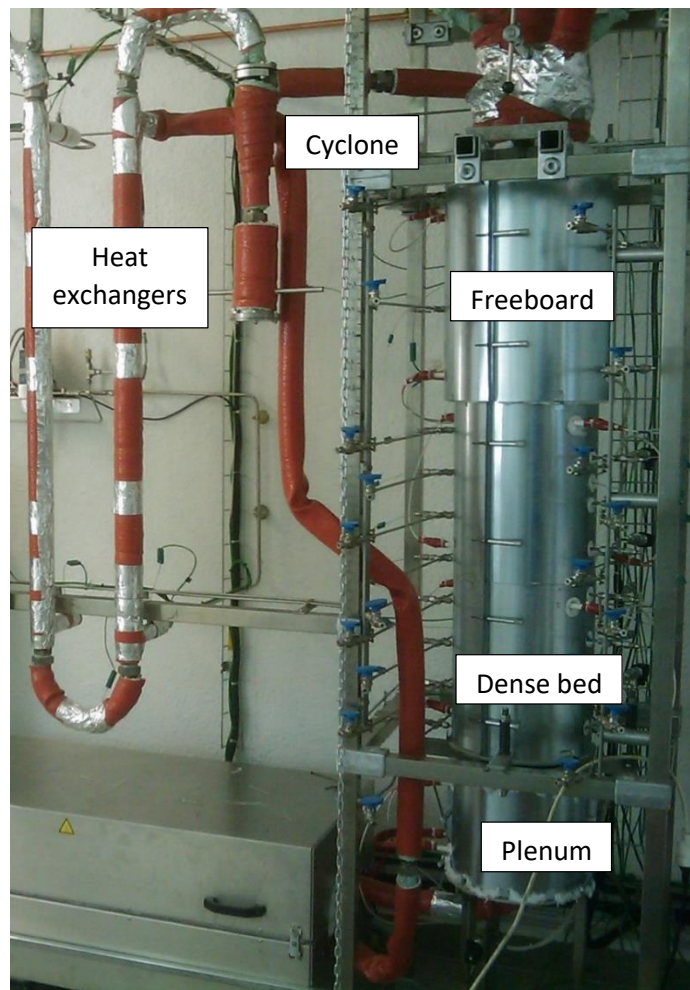
191 The SRF studied was provided by a French company of waste management and valorization.
192 It was selected as its composition was intermediate between biomass-rich SRF and plastic-rich
193 SRF. The same characterization methods were used for this SRF and for the Fly ashes
194 recovered in the cyclone after the experiments. The elemental composition was measured
195 according to the standard NF EN 15407. The ash content was measured at 550°C according to
196 the standard NF EN 15403. The composition of the resulting ashes was measured by X-Ray
197 Fluorescence Spectroscopy. Inductively Coupled Plasma – Atomic Emission Spectroscopy
198 (ICP-AES) was also used to characterize the mineral composition of the ashes after ash melting
199 (NF-M03-042). The SRF sample was calcined at 815°C, and the remaining ashes were melted
200 with $\text{Li}_2\text{B}_4\text{O}_7$ at 1000°C, before being dissolved in hydrochloric acid solution and detected by
201 AES detector. Finally, ionic chromatography was used to analyze the halogen compounds (NF
202 EN 1548 and NF EN ISO 10304-1).

203 The Lower Heating Value (LHV) of the SRF was measured with a calorimetric bomb (NF EN
204 15400). The proportion and composition of biomass, non-biomass, and inert materials were
205 determined according to the standard NF EN 15440 that is based on manual sorting.

206

207 **2.2 Gasification reactor and analysis of gas**

208 Gasification tests were performed in a bubbling fluidized-bed constructed at CNRS Nancy and
209 made of stainless steel 310 (Figure 1) [36, 78]. Briefly the gasifier is divided into three zones:
210 the plenum (d=100 mm, H=300 mm), the bed zone (d=100 mm, H=800 mm), and the freeboard
211 zone (d=140 mm, H=800 mm). The gasifying agent was air whose flow rate was controlled by
212 a mass flow controller (Brooks 5850S). At the bottom of the gasifier, a 3mm thick inox grid
213 was used as distributor plate to homogenize the air flow and insure an efficient fluidization.
214 The gasifier is heated by eight electrical heater shells at a maximum temperature of 1000 °C.



215

216

Fig. 1 Picture of the gasification unit

217 SRF were fed at the top of the reactor with a sloping screw. Around 3 kg of olivine was placed
218 in the gasifier. At 800°C, the minimum fluidization velocity (U_{mf}) was 0.15 m/s as measured
219 in this reactor by progressively increasing the air flowrate while measuring the pressure drop
220 in the gasifier (without SRF injection). This U_{mf} is in agreement with Cluet et al. [79]. At the
221 gasifier outlet, the syngas flowed through a cyclone to remove particles, before to be cooled
222 with two air heat exchangers. A water Venturi scrubber was also used to remove the tars and
223 the inorganic gases before flaring the syngas. The gasifier is equipped with 19 lateral tubes
224 allowing to insert thermocouples which locally measure the bed and freeboard temperatures.
225 Pressure was continuously measured below the grid and at the top of the freeboard zone.

226 The syngas was sampled before the Venturi scrubber and analyzed on-line by a μ -GC (Varian
227 micro-GC 490, 4 modules) every 3 minutes. N_2 , CO, CO_2 , H_2 , CH_4 , C_2H_2 , C_2H_4 , C_2H_6 , C_3H_4 ,
228 C_3H_6 , and C_6H_6 were quantified with this technique. To quantify the inorganic gases (H_2S ,
229 HCN, HCl and NH_3) present in syngas, the sampling procedure has been adapted from previous
230 articles [51, 54]. The analysis of the solutions was performed according to French and ISO
231 standards. 10 L of syngas was sampled in a Tedlar bag at the exit of the first heat exchanger.
232 Then, the syngas sampled in Tedlar bag was sequentially flowed at a constant flowrate (400
233 mL/min) during 5 minutes in impingers filled with 200 mL of specific solutions ([Table S.1 in](#)
234 [Supplementary Material](#)). The targeted ions S^{2-} (representing H_2S), Cl^- (representing HCl), and
235 NH_4^+ (representing NH_3) were analyzed by spectrophotometry, while the ion CN^- (representing
236 HCN) was quantified by ionic chromatography ([Table S.1 in Supplementary Material](#)).

237 238 [2.3 Gasification experimental protocol & performance indicators](#)

239 Before starting the gasification tests, the system was preheated at the desired temperature (750-
240 900 °C) under air. When the temperature was at the target value, the air flowrate was set at the
241 desired value. For all experiments, the air velocity was set at 4 times the minimum fluidization

242 velocity (thus 0.6 m/s), corresponding to an air flow rate of 4.5 m³/h (STP). Once the
243 temperatures were stable along the gasifier, the feeding of the SRF was started at a controlled
244 flowrate to reach the targeted equivalence ratio (ER). When the gasification conditions were
245 stable (gasifier temperature, and syngas composition analyzed by μ -GC), the steady-state
246 regime was maintained at least 40 minutes (Figure S.1 in supplementary material).

247 The ER is defined as the operating air flow rate divided by the air flow rate required for the
248 stoichiometric oxidation of SRF. In this study, the ER was varied between 0.18 and 0.27. The
249 effect of the ER on the gasification efficiency was studied at 800 °C (controlled by electrical
250 heater shells). To do so, the SRF flowrate was adjusted (between 4.67 to 6.95 kg/h) while the
251 air flow rate and the bed temperature were kept constant. In these conditions, the gas velocity
252 and residence time were similar for the different gasifying conditions. The SRF flow rate was
253 found to fluctuate by +/- 10% over time. For this reason, the ER range for each experimental
254 condition is presented in the results section. The SRF tank was continuously flushed with 10
255 L/min (STP) of pure N₂ to avoid the conversion of the fuel in the feeding screw. This flow rate
256 was taken into consideration for the results analysis since N₂ is used as a tracer for the
257 calculation of the syngas flowrate.

258 Four indicators of the gasification performance were used, namely: lower heating value of the
259 dry syngas (LHV_{syngas}), syngas yield (η_{syngas}), carbon conversion (CC), Cold Gas Efficiency
260 (CGE). Their determination based on experimental analysis was presented in a previous article
261 [78]. In these calculations, all the light hydrocarbon species (including benzene) were
262 considered as syngas components since their presence is not an issue for syngas valorization in
263 gas engine.

264 The lower heating value of the dry syngas (LHV_{syngas}), expressed in MJ/m³ (STP) of syngas
265 (including N₂), is calculated according to Eq.1:

266
$$\text{LHV}_{\text{syngas}} = \frac{\sum_i (x_i \text{LHV}_i)}{V_m} \quad \text{Eq.(1)}$$

267 Where V_m is the molar volume of ideal gas at STP (22.4 L/mol), and x_i the molar fraction of
 268 the gas species i .

269 The syngas yield (η_{syngas}) is calculated as the volume of dry syngas produced (including N_2) by
 270 kg of SRF (on dry ash free basis):

271
$$\eta_{\text{syngas}} = \frac{Q_{V_{\text{syngas}}}}{Q_{m_{\text{SRF}}}} \quad \text{Eq.(2)}$$

272 Where $Q_{V_{\text{syngas}}}$ is the volumetric syngas flowrate including N_2 (m^3/h STP) which is calculated
 273 using N_2 as a tracer, and $Q_{m_{\text{SRF}}}$ the mass flowrate of SRF ($\text{kg}_{\text{daf}}/\text{h}$).

274 The carbon conversion (CC) corresponds to the percentage of carbon transferred from SRF to
 275 syngas:

276
$$\text{CC} = Q_{m_{\text{syngas}}} M_C \frac{\sum_i \left(\frac{\omega_i}{M_i} n_i^C \right)}{Q_{m_{\text{SRF}}} X_C^{\text{SRF}}} \times 100 \quad \text{Eq.(3)}$$

277 Where $Q_{m_{\text{syngas}}}$ is the mass flowrate of syngas (kg/h), M_C is the molecular weight of carbon,
 278 n_i^C is the number of carbon atoms in the molecule i , X_C^{SRF} is the mass fraction of carbon in SRF
 279 (on daf basis), and ω_i and M_i correspond to the mass fraction of the gas i in the syngas and its
 280 molecular weight, respectively

281 Finally, the last indicator is the Cold Gas Efficiency (CGE) which reflects the fraction of
 282 chemical energy transferred from SRF to syngas:

283
$$\text{CGE} = \frac{\eta_{\text{syngas}} \text{LHV}_{\text{syngas}}}{\text{LHV}_{\text{SRF}}} \times 100 \quad \text{Eq.(4)}$$

284 In addition, the distribution of H atoms and C atoms in the gaseous products was calculated,
 285 according to Eq.(5) and (6):

286
$$S_H^i = \frac{n_H^i F^i}{\sum_k (n_H^k F^k)} \quad \text{Eq.(5)}$$

287
$$S_C^i = \frac{n_C^i F^i}{\sum_k (n_C^k F^k)} \quad \text{Eq.(6)}$$

288 Where S_H^i and S_C^i are the molar selectivity representing the molar flow rate of H (resp. C) atoms
289 present in a given molecule divided by the total flow rate of H (resp. C) atoms present in all
290 syngas molecules. F^i is the molar flowrate of a given molecule i .

291 **3. Results and discussion**

292 **3.1 Physico-chemical properties of the SRF**

293 The elemental composition of SRF is presented in **Table 1**. The carbon content is relatively low
294 (36.6 wt.%) while the ash content (35.1 wt.%) is significant compared to other SRFs reported
295 in the literature. Indeed, the carbon content usually ranges from 41 to 84 wt.% while the ash
296 content is in the range 1-27 wt.% [28, 30, 34, 48, 50, 54, 55, 80]. This composition results from
297 the production of SRF by mechanical-biological treatment of municipal solid waste. On the
298 contrary, the oxygen and hydrogen contents of this SRF are relatively lower than the reported
299 values. Mainly due to its high ash content, the LHV of the SRF (14.1 MJ/kg) is lower than the
300 values reported in the literature for SRFs (15-35 MJ/kg).

301 **Table 1** Elemental analysis and lower heating value of the SRF

Elemental analysis (dry wt.%)	
C	36.6
H	4.6
N	1.9
S	0.8
O (by difference)	21.1
Ash	35.1
LHV (MJ/kg_{dry})	14.1

302

303 The ash composition of the SRF is presented in **Table 2**. The main inorganic species are Si, Ca,
304 and Al. Alkaline and alkaline earth metals (AAEM, such as Mg, Na, K) are also present in the
305 ash composition. Some differences appear between ICP and XRF analysis. The SiO₂, Fe₂O₃,
306 and MnO contents are higher with ICP-AES measurement, while the CaO, TiO₂, and Na₂O₃
307 contents were higher with XRF analysis. ICP and XRF give similar values for Al₂O₃, MgO,
308 SO₃, P₂O₅. These results suggest that the characterization of complex wastes such as SRF must
309 be carefully performed and slight differences can be measured despite a rigorous sampling

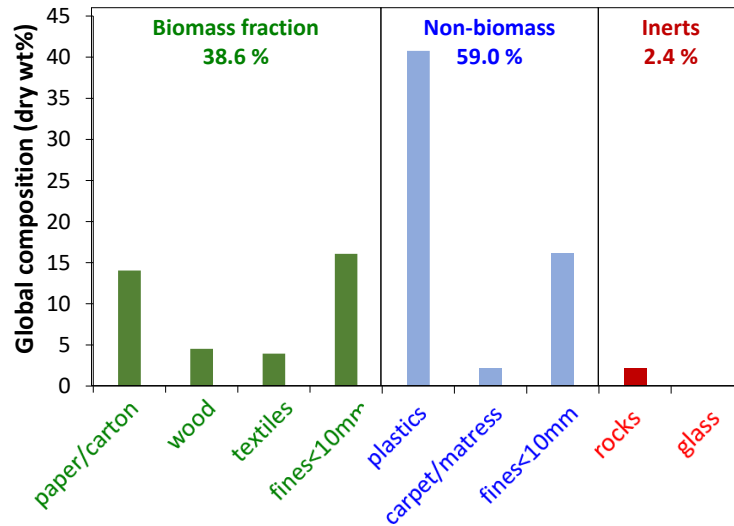
310 methodology. Regarding the potential inorganic gases release, it can be noted that the nitrogen
 311 and chlorine contents are lower than that of other SRFs studied in the literature (0.2-1.3 wt.%
 312 for N, and 0.7-1.1 wt.% for Cl) [30, 50, 54], whereas the sulphur content is slightly higher than
 313 the values reported in the literature (0-0.6 wt.%) [30, 31, 34, 48, 50, 54, 55].

314 **Table 2** Ash composition of the SRF measured by ICP-AES and XRF

Ash composition (in wt.%)		
	ICP-AES	XRF
SiO₂	41.5	30.8
Al₂O₃	10.5	10.5
Fe₂O₃	4.1	2.6
TiO₂	1.1	1.8
CaO	24.0	34.6
MgO	4.2	4.0
Na₂O	2.6	3.3
K₂O	0.9	0.5
SO₃	9.8	10.6
P₂O₅	1.0	1.0
MnO	0.2	0.1
Total	100.0	100.0
Br	<i>nd</i>	
Cl	0.30	
F	0.04	

315 **Figure 2** shows the proportion and composition of biomass, non-biomass, and inert fractions
 316 composing the SRF. Our previous article presented the effect of operating conditions on
 317 gasification efficiency for two SRFs (one rich in biomass and glass, and a second richer in
 318 plastics) [78]. Herein we complete our previous study with another SRF which exhibits an
 319 interesting composition between biomass-rich SRF and plastic-rich SRF. Indeed, this sample
 320 is composed of non-biomass (59.0 wt.%), biomass (38.6 wt.%), and inert (2.4 wt.%) fractions.
 321 The non-biomass fraction is rich in plastics, while the biomass fraction is mainly composed of
 322 paper/carton. Significant parts of these fractions are composed of fines for which the origin has
 323 not been identified and that may contain ash-rich materials. This would explain the high ash
 324 content of this SRF (35.1 wt.%), whereas the inert fraction is low (2.4 wt.%). This inert fraction

325 is only composed of rocks (not glass). It must be noted that the SRF composition strongly
 326 depends on the origin of the collected wastes and on the sorting methods used by the waste
 327 treatment plant.



328

329 **Fig. 2** Proportion and composition of biomass, non-biomass, and inert materials in the SRF

330 **3.2 Permanent gases composition**

331 **3.2.1 Influence of the temperature**

332 The values of the cold gas efficiency (CGE), the carbon conversion (CC), the syngas yield
 333 (η_{syngas}) and the lower heating value of the syngas ($\text{LHV}_{\text{syngas}}$) obtained during the gasification
 334 tests are presented in **Table 3**. It can be noted that the temperature increase from 750 to 800 °C
 335 does not significantly modify the gasification results. However, at 900 °C, all the gasification
 336 indicators are strongly improved. The combined increase in $\text{LHV}_{\text{syngas}}$ (+4.5%) and η_{syngas}
 337 (+10%) result in an overall gain of 13% for the CGE (from 74.5 to 84.3 %). The temperature
 338 increase also promotes the carbon conversion (+6%). Some explanations are given thereafter.

339

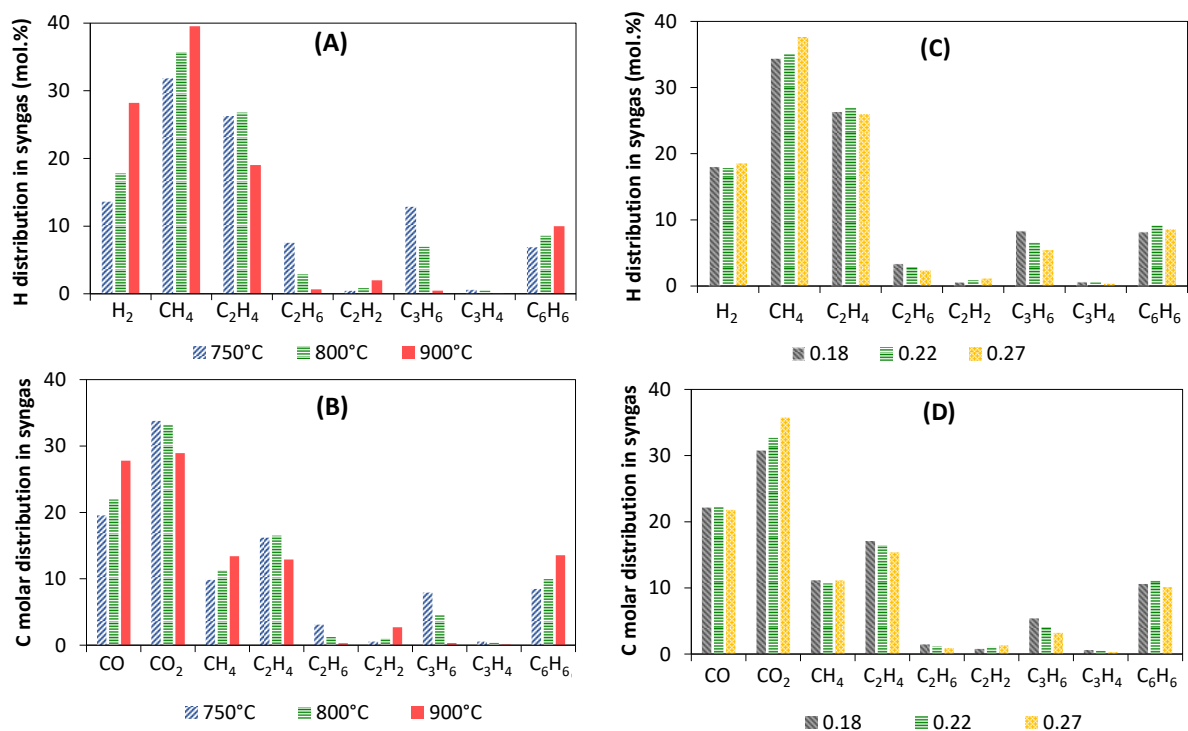
340 **Table 3** Operating conditions and results of the gasification tests performed at different
 341 temperatures and ER=0.22 (ranging between 0.205 and 0.227), and at different Equivalent
 342 Ratio (ER) and a Temperature of 803°C

T (°C)	Influence of T			Influence of ER		
	750	803	902	803	803	803
Equivalence Ratio	0.22 (0.205- 0.227)	0.22 (0.205- 0.227)	0.22 (0.205- 0.227)	0.18 (0.170- 0.188)	0.22 (0.205- 0.227)	0.27 (0.253- 0.279)
Syngas composition (%vol.)						
N₂	59.6	57.7	54.1	53.7	57.7	63.0
H₂	4.0	5.0	8.7	5.8	5.0	4.5
CO	9.3	10.3	12.6	11.0	10.3	8.8
CO₂	16.0	15.1	13.2	15.2	15.1	14.5
CH₄	4.7	4.9	6.1	5.5	4.9	4.5
C₂H₄	3.8	3.8	2.9	4.2	3.8	3.1
C₂H₆	0.7	0.3	0.1	0.4	0.3	0.2
C₂H₂	0.1	0.3	0.6	0.2	0.3	0.3
C₃H₆	1.3	0.6	0.1	0.9	0.6	0.4
C₃H₄	0.1	0.1	0.0	0.1	0.1	0.0
C₆H₆	0.7	0.9	1.0	0.9	0.9	0.7
LHV_{syngas} (MJ/m³ STP)	7.97	8.05	8.38	9.1	8.05	6.7
η_{syngas} (m³ STP/kgSRF daf)	2.00	2.06	2.20	1.84	2.06	2.33
Carbon conversion (%)	88.4	90.3	94.9	86.7	90.3	89.9
Cold Gas Efficiency (%)	73.0	76.2	84.3	77.0	76.2	71.7

343 In the literature, similar trends were reported, where rising gasification temperature at constant
 344 ER promoted the syngas yield and carbon conversion[38]. However, a significant discrepancy
 345 was reported in the literature for the evolution of CGE and LHV_{syngas}, since they were reported
 346 to decrease with increasing temperature [50, 54]. It has to be stressed out that, at industrial
 347 scale, such a temperature rise in the gasifier is obtained by increasing the ER resulting in higher
 348 syngas oxidation. In our case, ER is varied by maintaining a constant temperature thanks to the
 349 heating of the reactor walls.

350 The evolution of the syngas composition (Table 3) explains the increase in calorific value with
351 rising temperature. Indeed, H₂, CO, CH₄, C₂H₂, and C₆H₆ contents significantly increase at 900
352 °C, while CO₂ is substantially reduced. High temperature is known to promote char gasification
353 reaction leading to the production of H₂ and CO [78]. H₂ and CO formation at elevated
354 temperature can also result from tar decomposition by cracking, as well as steam and dry
355 reforming [30, 50, 54]. Dry reforming reaction can contribute to the decrease of CO₂ with
356 increasing temperature. This set of reactions is responsible for the evolution of syngas
357 composition and gasification efficiency with rising temperature.

358 It can be highlighted that, despite the high ash content, no melting phenomenon leading to bed
359 defluidization and agglomeration were observed under these operating conditions. Compared
360 with syngas produced by miscanthus air gasification in the same reactor under similar operating
361 conditions [36], the syngas produced in this study has lower content of H₂ and CO, while the
362 content in CH₄ and small hydrocarbon compounds (especially C₂H₄) is significantly higher.
363 This high content in hydrocarbon compounds is explained by the presence of plastics which
364 are known to produce high content in CH₄ and C₂-C₃ compounds during gasification [48, 55,
365 78].



366

367

Fig. 3 Distribution of hydrogen and carbon atoms in syngas species as function of

368

gasification temperature on (A) and (B), and of ER on (C) and (D).

369

The influence of the temperature on the distribution of hydrogen and carbon atoms in the

370

gaseous products is presented in Figure 3-A and B, respectively. The main H-containing

371

species is CH₄ (Figure 3-A), resulting from the decomposition of tar compounds [81–83].

372

Rising temperature increases the selectivity in H₂, especially at temperature higher than 800

373

°C. At the same time, the selectivity in light hydrocarbons (C₂H₄, C₂H₆, C₃H₆, and C₃H₄)

374

remarkably decreases. C₂H₂ increases mainly from other C₂ conversion [84]. These results

375

confirm that light hydrocarbons are considerably reformed to H₂ and CO in the gasification

376

process when the temperature increases.

377

The carbon atoms distribution shows that the most important species are:

378

CO₂>CO>C₂H₄>CH₄>C₆H₆ (Figure 3-B). C₆H₆ is a stable tertiary product not converted in our

379

conditions [83, 85]. A decrease in CO₂ is observed at 900°C, together with an increase in CO,

380

C₆H₆, and CH₄. These evolutions suggest that dry reforming reactions are promoted at high

381 temperature [86]. The increase in temperature promotes the kinetics of reactions (water gas
382 shift, hydrocarbons reforming, etc.) but also modifies the thermodynamic equilibrium of the
383 reactive system. We have previously studied the effect of temperature on the detailed
384 mechanisms of syngas conversion. We have especially shown that OH radicals are mainly
385 produced by CO₂ conversion ($\text{CO}_2 + \text{H} = \text{CO} + \text{OH}$) in a syngas [84]. Therefore, under air
386 gasification conditions, CO₂ yields are controlled by the competition between oxidation
387 reactions (producing CO₂) and CO₂ conversion in the gas phase. In comparison with syngas
388 produced in the same reactor under similar operating conditions with other types of SRF [78],
389 the syngas produced by this SRF presents a CO₂ and CO contents significantly lower, while
390 the content in CH₄ and C₂H₄, and mainly C₃H₆ are higher. The low content of CO and CO₂
391 results from the low O/C ratio in the plastic contained in SRF, as clearly explained by *Valin et*
392 *al.* [38]. The high content in C₃H₆ with this SRF is expected to result from the fast
393 decomposition of polymer chains of the plastics contained in this SRF, and to the low catalytic
394 activity of olivine towards tar reforming reactions due to poisoning of active sites with
395 inorganic gases [55].

396 *3.2.2 Influence of the Equivalence Ratio*

397 The evolutions of the gasification indicators with increasing ER are presented in [Table 3](#). It can
398 be observed that increasing ER results in a decrease of the CGE, a significant increase in syngas
399 yield, and a drastic drop of the LHV_{syngas}. While oxidation reactions are expected to increase
400 with higher ER, the carbon conversion is almost stable between ER=0.22 and 0.27. The large
401 amount of inorganic species known for their catalytic activity (such as Ca, Na, K or Fe) could
402 catalyze the gasification reactions of the carbonaceous solids and promote the carbon
403 conversion even at low ER [87]. Nevertheless, approximately 10 to 13 wt.% of the carbon
404 inlet was not converted. Most of this non-converted carbon was supposed to be recovered in
405 the form of fly ash and tar compounds. The elemental composition of the fly ash was analyzed.

406 Whatever the ER value, it consists mainly in ash (~87 wt.%), carbon (~12 wt.%), low amounts
407 of hydrogen (~0.7 wt.%) and nitrogen (~0.5 wt.%). During the gasification at 800°C, the fly
408 ash yield was 16 wt.%. Thus, the fly ash contains 5.5 wt.% of the carbon input. This result
409 confirms that part of the carbon input is not converted during gasification and is recovered in
410 the form of fly ash. This results exemplifies the important effect of particles elutriation on the
411 carbon balance [88].

412 The increase in syngas yield with rising ER is explained by the higher ratio of air to SRF in the
413 gasifier, leading to a higher dilution of the syngas produced into N₂ from air. To better
414 understand the effects of increasing ER on the syngas produced, the syngas yield and the
415 LHV_{syngas} have been calculated for N₂-free syngas (Figure S.2 in Supplementary Material). The
416 results demonstrate that LHV_{syngas} of N₂-free syngas sharply decreases with increasing ER.
417 Simultaneously, the syngas yield was shown to be almost invariant with rising ER. As a result,
418 increasing ER results in the decrease of CGE.

419 Table 3 presents the syngas composition at the gasifier outlet (including N₂), while Figure S.3
420 (in supplementary material) displays the composition of the gas produced by gasification
421 without nitrogen. Rising ER decreases the fraction of the produced gases, except for CO₂ which
422 is generated by the oxidation reactions promoted by high ER. Indeed, syngas and char can both
423 be oxidized with increasing ER. The syngas oxidation reactions also explain the decrease of
424 the LHV_{syngas} with rising ER (Figure S.2). The syngas yield is not impacted by the ER variation
425 under the actual conditions of this study. These trends are similar to that obtained during
426 miscanthus gasification in the same reactor under similar operating conditions [36].

427 The distribution of hydrogen and carbon atoms in the syngas was also investigated. The results,
428 presented in Figure 3-C and D, reveal that the distribution is poorly modified with rising ER.
429 For H atoms distribution, the selectivity in CH₄ and C₆H₆ slightly increases with rising ER,

430 while that of C_3H_6 and C_2H_6 decreases. Indeed, CH_4 and C_6H_6 are known to be more stable
431 hydrocarbons than C_3H_6 and C_2H_6 [89, 90]. Regarding the carbon atoms distribution, the main
432 effect of rising ER consists in increasing the CO_2 selectivity. Thus, hydrocarbon molecules
433 (notably C_2H_4 and C_3H_6 , based on C atoms molar distribution) seem to be oxidized into CO_2
434 when the ER increases. The higher increase in CO_2 compared to H_2 (and CO) in terms of molar
435 distribution in C or H atoms shows that higher ER promotes CO_2 (and not CO) and that steam
436 reforming reactions are not significantly promoted by ER under our conditions.

437 Compared with results obtained in the same reactor under similar operating conditions with
438 other types of SRF [78], higher carbon conversion and LHV were obtained with the present
439 SRF. As a result, the CGE is higher than that obtained with a SRF rich in paper and another
440 mostly composed of plastics (SRF1 and SRF2 of the previous article [78]). Thus, the mixture
441 of soft plastics with ash-containing waste in this SRF seems to promote the gasification
442 efficiency.

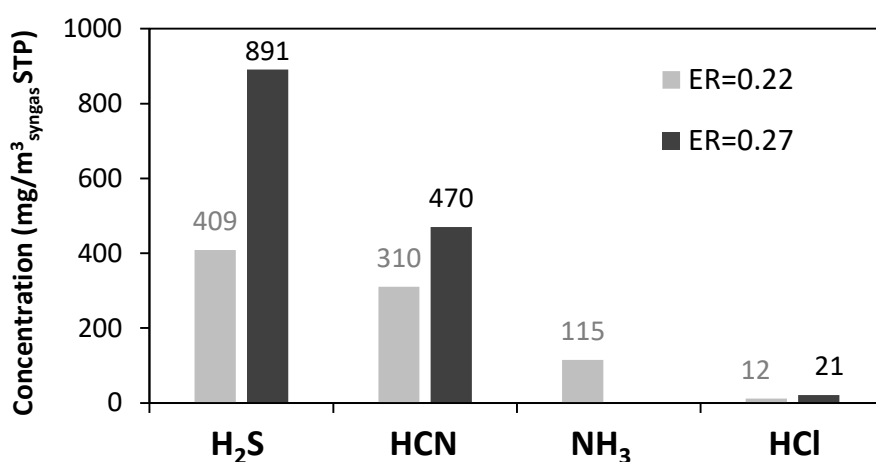
443 3.3 Inorganic gases composition

444 As explained in the introduction, conflicting results are presented in the literature about the
445 effect of ER on the release of inorganic gases. To investigate this phenomenon, the
446 concentrations of H₂S, HCl, NH₃ and HCN were measured at two different ER in this study:
447 0.22 and 0.27. In addition, fly ash and bed material after gasification were analyzed. Since the
448 solid samples recovered were generated in different operating conditions (constant temperature
449 but different ER), the results are only qualitative and are presented in supplementary material.

450 The results of inorganic gases analysis (presented in [Figure 4](#)) show that H₂S is the most
451 important inorganic gas generated during the gasification of this SRF. Its content increases
452 from 409 to 891 mg/Nm³ of syngas with increasing ER. These values correspond respectively
453 to 11% and 26% of the sulfur contained in the SRF. These values are in agreement with *Pinto*
454 *et al.* [31], while *Valin et al.* reported that 45 to 65% of sulfur was transformed into H₂S during
455 SRF air gasification [38]. To better understand the sulfur species distribution, the sulfur content
456 of fly ash and bed materials after gasification were qualitatively analyzed in this study
457 (Supplementary Material). Strong interactions between the olivine bed (containing iron) and
458 H₂S are expected to immobilize the produced H₂S in the fluidized bed during SRF gasification,
459 while a lower amount of H₂S seems to be adsorbed on the fly ash due to the presence of AAEM
460 species and iron. Other species not analyzed in this study, such as tar molecules (thiophene,
461 benzo- and dibenzo-thiophene, thiols, or aryl and alkyl-sulphides) could also contain part of
462 the sulfur [31].

463 For nitrogenous gases, both HCN and NH₃ are generated at low ER. However, at ER=0.27, no
464 ammonia is detected in the syngas, whereas HCN concentration increases. HCN is typically
465 generated by the decomposition of nitrogenous polymers [61]. The significant plastic content
466 in this SRF may explain the production of HCN. The NH₃ and HCN contents are in agreement

467 with previous studies dealing with SRF gasification [34, 50, 54], where HCN content was found
 468 to vary from 27 to 660 mg/Nm³ and NH₃ from 0 to 200 mg/Nm³. Anyway, these HCN and
 469 NH₃ content correspond to a very small part of the N present in the SRF (less than 6 %). The
 470 formation of other N-gases (such as N₂, NO_x) [39, 57], and condensable compounds (cyano-
 471 acetylene, acetonitrile, isoquinoline, indole, carbazole, quinoline, other N-heteroaromatic
 472 compounds) [49, 57, 91, 92] can explain this difference. It should be noted that the formation
 473 of N₂ is really difficult to assess since it would be highly diluted in the N₂ that comes from air.
 474 In addition, part of the syngas water could have condensed in the Tedlar bag during sampling,
 475 possibly leading to NH₃ dissolution [93]. Nevertheless, no trace of condensation was observed
 476 in the Tedlar bag during experiments. Qualitative distribution of nitrogen compounds presented
 477 in Supplementary Material highlights that the majority of N-compounds was not identified in
 478 this study. This issue was also reported by other authors [38].



479

480 **Fig. 4** Influence of the ER on the inorganic gases concentration at T=800°C

481 The content of HCl in the syngas is low compared both to the other inorganic gases and to the
 482 data available in the literature [30, 54]. This result can be explained by the low Cl content in
 483 this SRF (0.3 wt.%). But even at ER=0.27, HCl represents less than 2% of the chlorine present
 484 in the SRF. An explanation is that there are reactions occurring between HCl and the AAEM

485 species of SRF removing HCl from the syngas [68, 94]. The qualitative analysis of fly ash and
486 bed material presented in Supplementary Material implies that chlorine is mainly trapped in
487 the fly ash after gasification.

488 These results support the observation of several researchers suggesting that rising ER increases
489 the inorganic gases content in the syngas [31, 49, 95]. It may be due to the fact that high ER
490 promotes the char gasification reactions thus enhancing the release of heteroatoms, but in the
491 results presented in Table 3, the carbon conversion is stable when ER increases from 0.22 to
492 0.27. This stability is not logical and seems suspicious since rising ER in such a range is
493 expected to increase the carbon conversion [78]. The values for inorganic gases obtained in
494 this study are in agreement with the range of available data in the literature [30, 50, 54, 55].

495 The inorganic gases contents are significantly higher than the standard required for syngas
496 valorization in gas engine. The maximum acceptable values are around 100 mg/m³ for H₂S, 50
497 mg/m³ for NH₃, and 9 mg/m³ for HCl [32, 39]. These results confirm that inorganic gases are
498 an important issue for the SRF gasification.

499 **4. Conclusions**

500 This article studied air gasification of an industrial Solid Recovered Fuel in allothermal
501 bubbling fluidized bed. Since the valorization of low-grade SRF by gasification processes
502 could be jeopardized by the low quality of the resulting syngas, the syngas composition was
503 deeply analyzed in this study.

504 Increasing gasification temperature from 750 to 800°C had low effect on gasification, while
505 drastic improvement of gasification efficiency and syngas quality was observed at 900°C. This
506 beneficial effect was attributed to the promotion of secondary reactions (including
507 hydrocarbons conversion) and char gasification. The influence of equivalence ratio (ER) was
508 significantly less important than temperature on the gasification efficiency. The main effect

509 consisted in the decrease of the syngas LHV due to the promotion of oxidation reactions. As a
510 result, the CO₂ content was found to increase while the CGE decreased.

511 The high content in light hydrocarbon compounds (CH₄, C₂H₄, C₃H₆) with this SRF resulted
512 from the fast decomposition of polymer chains of the plastics contained in this SRF, and to the
513 low catalytic activity of olivine towards tar reforming reactions due to poisoning of active sites
514 with inorganic gases (HCl, H₂S). Compared with results obtained in the same reactor under
515 similar operating conditions with other types of SRF, the gasification efficiency with the
516 present SRF was higher than those obtained with a SRF rich in paper and another mostly
517 composed of plastics. Thus, the mixture of soft plastics with ash-containing waste in this SRF
518 seems to promote the gasification efficiency.

519 The concentration of H₂S, HCl, NH₃ and HCN in the syngas produced at 800°C was measured
520 at two different ER (0.22 and 0.27). Both HCN and NH₃ were generated at low ER. However,
521 at ER=0.27, no ammonia was recovered in the syngas, whereas HCN concentration increased.
522 The significant plastic content in this SRF may explain the release of HCN. The nitrogen mass
523 inventory was low, reflecting that most of nitrogen compounds were not detected in the form
524 of NH₃ or HCN. The HCl content in syngas was low compared to the data available in the
525 literature, due to the low Cl content in the SRF (0.3 wt.%) and to the immobilization of Cl in
526 the fly ash containing K and Ca. H₂S was the most important inorganic gas and its content
527 increased with increasing ER : from 409 to 891 mg/m³ STP at ER=0.22 and 0.27, respectively.
528 These values correspond to 11% and 26% of the sulfur present in SRF, while part of sulfur was
529 expected to react with the olivine bed.

530 Even if the S, N and Cl present in the SRF are not converted completely into inorganic gases,
531 the concentrations of H₂S, NH₃ and HCl are too high in comparison with the maximum
532 acceptable values for syngas valorization in gas engine. Qualitative analysis of fly ash and

533 olivine bed after gasification tests proved that interactions between these materials and
534 inorganic gases occur allowing to limit the inorganic gases production. More work is needed
535 to deeply understand the exact nature of the gasification products that contained S, N and Cl,
536 as well as to optimize waste mixture composition in SRF to promote interactions between
537 inorganic gases and fly ash/bed material in order to limit the presence of inorganic gases in the
538 gasifier.

539 Acknowledgements

540 The authors acknowledge the financial support of ADEME, France –Terracotta project, n°
541 1606C0013. The authors also thank the EDF Company, France, especially Emmanuel Thunin
542 and Mathieu Insa for their support on material characterizations, as well as Matthieu Debal,
543 Pierre Girods and Yann Rogaume (LERMAB, University de Lorraine) for their tremendous
544 work for SRF pelletization.

545 References

- 546 1. Kaza, S., Yao, L., Bhada-Tata, P., Van Woerden, F.: What a waste 2.0: A global Snapshot of Solid
547 Waste Management to 2050. , Washington, DC (2018)
- 548 2. Kang, P., Zhang, H., Duan, H.: Characterizing the implications of waste dumping surrounding
549 the Yangtze River economic belt in China. *J. Hazard. Mater.* 383, 121207 (2020).
550 <https://doi.org/10.1016/j.jhazmat.2019.121207>
- 551 3. Hafeez, S., Mahmood, A., Syed, J.H., Li, J., Ali, U., Malik, R.N., Zhang, G.: Waste dumping sites as
552 a potential source of POPs and associated health risks in perspective of current waste
553 management practices in Lahore city, Pakistan. *Sci. Total Environ.* 562, 953–961 (2016).
554 <https://doi.org/10.1016/j.scitotenv.2016.01.120>
- 555 4. Rego, R.F., Moraes, L.R.S., Dourado, I.: Diarrhoea and garbage disposal in Salvador, Brazil.
556 *Trans. R. Soc. Trop. Med. Hyg.* 99, 48–54 (2005). <https://doi.org/10.1016/j.trstmh.2004.02.008>
- 557 5. Kupchik, G.J., Franz, G.J.: Solid Waste, Air Pollution and Health. *J. Air Pollut. Control Assoc.* 26,
558 116–118 (1976). <https://doi.org/10.1080/00022470.1976.10470229>
- 559 6. Triassi, M., Alfano, R., Illario, M., Nardone, A., Caporale, O., Montuori, P., Triassi, M., Alfano, R.,
560 Illario, M., Nardone, A., Caporale, O., Montuori, P.: Environmental Pollution from Illegal Waste
561 Disposal and Health Effects: A Review on the “Triangle of Death.” *Int. J. Environ. Res. Public*.
562 *Health.* 12, 1216–1236 (2015). <https://doi.org/10.3390/ijerph120201216>
- 563 7. Plaza, P.I., Lambertucci, S.A.: How are garbage dumps impacting vertebrate demography,
564 health, and conservation? *Glob. Ecol. Conserv.* 12, 9–20 (2017).
565 <https://doi.org/10.1016/j.gecco.2017.08.002>
- 566 8. Schweitzer, L., Noblet, J.: Chapter 3.6 - Water Contamination and Pollution. In: Török, B. and
567 Dransfield, T. (eds.) *Green Chemistry*. pp. 261–290. Elsevier (2018)
- 568 9. Lebreton, L., Slat, B., Ferrari, F., Sainte-Rose, B., Aitken, J., Marthouse, R., Hajbane, S., Cunsolo,
569 S., Schwarz, A., Levivier, A., Noble, K., Debeljak, P., Maral, H., Schoeneich-Argent, R., Brambini,
570 R., Reisser, J.: Evidence that the Great Pacific Garbage Patch is rapidly accumulating plastic. *Sci.*
571 *Rep.* 8, 4666 (2018). <https://doi.org/10.1038/s41598-018-22939-w>
- 572 10. Haward, M.: Plastic pollution of the world’s seas and oceans as a contemporary challenge in
573 ocean governance. *Nat. Commun.* 9, 667 (2018). <https://doi.org/10.1038/s41467-018-03104-3>
- 574 11. Solid Waste Management,
575 <http://www.worldbank.org/en/topic/urbandevelopment/brief/solid-waste-management>
- 576 12. Martignon, G., Edo, M.: Trends on use of solid recovered fuels. IEA Bioenergy (2020)
- 577 13. Vonk, G., Piriou, B., Wolbert, D., Cammarano, C., Vaïtilingom, G.: Analysis of pollutants in the
578 product gas of a pilot scale downdraft gasifier fed with wood, or mixtures of wood and waste
579 materials. *Biomass Bioenergy.* 125, 139–150 (2019).
580 <https://doi.org/10.1016/j.biombioe.2019.04.018>

- 581 14. Combustibles solides de récupération (CSR) - Caractérisation et évaluation de leurs
582 performances en combustion. FEDEREC et COMPTE-R (2015)
- 583 15. Consommation d'énergie primaire - Eurostat, [https://ec.europa.eu/eurostat/fr/web/products-](https://ec.europa.eu/eurostat/fr/web/products-datasets/-/T2020_33)
584 [datasets/-/T2020_33](https://ec.europa.eu/eurostat/fr/web/products-datasets/-/T2020_33)
- 585 16. Brunner, P.H., Morf, L., Rechberger, H.: VI.3 - Thermal waste treatment – a necessary element
586 for sustainable waste management. In: Twardowska, I. (ed.) Waste Management Series. pp.
587 783–806. Elsevier (2004)
- 588 17. Porteous, A.: Why energy from waste incineration is an essential component of
589 environmentally responsible waste management. *Waste Manag.* 25, 451–459 (2005).
590 <https://doi.org/10.1016/j.wasman.2005.02.008>
- 591 18. Arena, U.: Process and technological aspects of municipal solid waste gasification. A review.
592 *Waste Manag.* 32, 625–639 (2012). <https://doi.org/10.1016/j.wasman.2011.09.025>
- 593 19. Enerkem produces renewable alternative solution to diesel fuel. *Focus Catal.* 2018, 6 (2018).
594 <https://doi.org/10.1016/j.focat.2018.11.097>
- 595 20. Barba, A., Le Cadre, E., Forsgren, H., Gaillard, M., Gunnarsson, I., Guerrini, O., Hoff, M.V., Kara,
596 Y., Mollema, E., Moretti, I., Ourliac, M., Overwijk, M., Peureux, G., Peltenburg, A., Tengberg, F.,
597 De Vries, T., Winjstra, S.: Europe move towards industrialization of 2G biomethane from
598 biomass gasification and methanation. Presented at the International Gas Research
599 Conference Proceedings (2017)
- 600 21. Ramos, A., Monteiro, E., Silva, V., Rouboa, A.: Co-gasification and recent developments on
601 waste-to-energy conversion: A review. *Renew. Sustain. Energy Rev.* 81, 380–398 (2018).
602 <https://doi.org/10.1016/j.rser.2017.07.025>
- 603 22. Sansaniwal, S.K., Pal, K., Rosen, M.A., Tyagi, S.K.: Recent advances in the development of
604 biomass gasification technology: A comprehensive review. *Renew. Sustain. Energy Rev.* 72,
605 363–384 (2017). <https://doi.org/10.1016/j.rser.2017.01.038>
- 606 23. Campoy, M., Gómez-Barea, A., Ollero, P., Nilsson, S.: Gasification of wastes in a pilot fluidized
607 bed gasifier. *Fuel Process. Technol.* 121, 63–69 (2014).
608 <https://doi.org/10.1016/j.fuproc.2013.12.019>
- 609 24. Karatas, H., Olgun, H., Engin, B., Akgun, F.: Experimental results of gasification of waste tire
610 with air in a bubbling fluidized bed gasifier. *Fuel.* 105, 566–571 (2013).
611 <https://doi.org/10.1016/j.fuel.2012.08.038>
- 612 25. Xiao, G., Ni, M.-J., Chi, Y., Cen, K.-F.: Low-temperature gasification of waste tire in a fluidized
613 bed. *Energy Convers. Manag.* 49, 2078–2082 (2008).
614 <https://doi.org/10.1016/j.enconman.2008.02.016>
- 615 26. Di Gregorio, F., Santoro, D., Arena, U.: The effect of ash composition on gasification of poultry
616 wastes in a fluidized bed reactor. *Waste Manag. Res.* 32, 323–330 (2014).
617 <https://doi.org/10.1177/0734242X14525821>
- 618 27. Mastellone, M.L., Zaccariello, L., Arena, U.: Co-gasification of coal, plastic waste and wood in a
619 bubbling fluidized bed reactor. *Fuel.* 89, 2991–3000 (2010).
620 <https://doi.org/10.1016/j.fuel.2010.05.019>
- 621 28. Arena, U., Di Gregorio, F.: Energy generation by air gasification of two industrial plastic wastes
622 in a pilot scale fluidized bed reactor. *Energy.* 68, 735–743 (2014).
623 <https://doi.org/10.1016/j.energy.2014.01.084>
- 624 29. Wilk, V., Hofbauer, H.: Co-gasification of Plastics and Biomass in a Dual Fluidized-Bed Steam
625 Gasifier: Possible Interactions of Fuels. *Energy Fuels.* 27, 3261–3273 (2013).
626 <https://doi.org/10.1021/ef400349k>
- 627 30. Dunnu, G., Panopoulos, K.D., Karellas, S., Maier, J., Toulou, S., Koufodimos, G., Boukis, I.,
628 Kakaras, E.: The solid recovered fuel Stabilat®: Characteristics and fluidised bed gasification
629 tests. *Fuel.* 93, 273–283 (2012). <https://doi.org/10.1016/j.fuel.2011.08.061>
- 630 31. Pinto, F., André, R.N., Carolino, C., Miranda, M., Abelha, P., Direito, D., Perdikaris, N., Boukis, I.:
631 Gasification improvement of a poor quality solid recovered fuel (SRF). Effect of using natural

- 632 minerals and biomass wastes blends. *Fuel*. 117, 1034–1044 (2014).
 633 <https://doi.org/10.1016/j.fuel.2013.10.015>
- 634 32. Milne, T.A., Evans, R.J., Abatzoglou, N.: Biomass Gasifier Tars: Their Nature, Formation and
 635 Conversion. National Renewable Energy Laboratory (1998)
- 636 33. Vonk, G., Piriou, B., Felipe Dos Santos, P., Wolbert, D., Vaïtilingom, G.: Comparative analysis of
 637 wood and solid recovered fuels gasification in a downdraft fixed bed reactor. *Waste Manag.*
 638 85, 106–120 (2019). <https://doi.org/10.1016/j.wasman.2018.12.023>
- 639 34. Arena, U., Di Gregorio, F.: Gasification of a solid recovered fuel in a pilot scale fluidized bed
 640 reactor. *Fuel*. 117, 528–536 (2014). <https://doi.org/10.1016/j.fuel.2013.09.044>
- 641 35. Recari Ansa, J.: Gasification of biomass and solid recovered fuels (SRFs) for the synthesis of
 642 liquid fuels, (2017)
- 643 36. Lardier, G., Kaknics, J., Dufour, A., Michel, R., Cluet, B., Authier, O., Poirier, J., Mauviel, G.: Gas
 644 and Bed Axial Composition in a Bubbling Fluidized Bed Gasifier: Results with Miscanthus and
 645 Olivine. *Energy Fuels*. 30, 8316–8326 (2016). <https://doi.org/10.1021/acs.energyfuels.6b01816>
- 646 37. Horvat, A., Kwapinska, M., Xue, G., Rabou, L.P.L.M., Pandey, D.S., Kwapinski, W., Leahy, J.J.:
 647 Tars from Fluidized Bed Gasification of Raw and Torrefied Miscanthus x giganteus. *Energy*
 648 *Fuels*. 30, 5693–5704 (2016). <https://doi.org/10.1021/acs.energyfuels.6b00532>
- 649 38. Valin, S., Ravel, S., Pons de Vincent, P., Thiery, S., Miller, H.: Fluidized bed air gasification of
 650 solid recovered fuel and woody biomass: Influence of experimental conditions on product gas
 651 and pollutant release. *Fuel*. 242, 664–672 (2019). <https://doi.org/10.1016/j.fuel.2019.01.094>
- 652 39. Woolcock, P.J., Brown, R.C.: A review of cleaning technologies for biomass-derived syngas.
 653 *Biomass Bioenergy*. 52, 54–84 (2013). <https://doi.org/10.1016/j.biombioe.2013.02.036>
- 654 40. Torres, W., Pansare, S.S., Jr, J.G.G.: Hot Gas Removal of Tars, Ammonia, and Hydrogen Sulfide
 655 from Biomass Gasification Gas. *Catal. Rev.* 49, 407–456 (2007).
 656 <https://doi.org/10.1080/01614940701375134>
- 657 41. Asadullah, M.: Biomass gasification gas cleaning for downstream applications: A comparative
 658 critical review. *Renew. Sustain. Energy Rev.* 40, 118–132 (2014).
 659 <https://doi.org/10.1016/j.rser.2014.07.132>
- 660 42. GE Jenbacher: Fuel gas quality, special gases. (2009)
- 661 43. Gupta, R.P., Turk, B.S., Portzer, J.W., Cicero, D.C.: Desulfurization of syngas in a transport
 662 reactor. *Environ. Prog.* 20, 187–195 (2001)
- 663 44. Lee, J., Feng, B.: A thermodynamic study of the removal of HCl and H₂S from syngas. *Front.*
 664 *Chem. Sci. Eng.* 6, 67–83 (2012). <https://doi.org/10.1007/s11705-011-1162-4>
- 665 45. Tijmensen, M.J.A., Faaij, A.P.C., Hamelinck, C.N., van Hardeveld, M.R.M.: Exploration of the
 666 possibilities for production of Fischer Tropsch liquids and power via biomass gasification.
 667 *Biomass Bioenergy*. 23, 129–152 (2002). [https://doi.org/10.1016/S0961-9534\(02\)00037-5](https://doi.org/10.1016/S0961-9534(02)00037-5)
- 668 46. Chiche, D., Diverchy, C., Lucquin, A.-C., Porcheron, F., Defoort, F.: Synthesis Gas Purification. *Oil*
 669 *Gas Sci. Technol. – Rev. D’IFP Energ. Nouv.* 68, 707–723 (2013).
 670 <https://doi.org/10.2516/ogst/2013175>
- 671 47. Kaufman Rechulski, M.D., Schildhauer, T.J., Biollaz, S.M.A., Ludwig, Ch.: Sulfur containing
 672 organic compounds in the raw producer gas of wood and grass gasification. *Fuel*. 128, 330–339
 673 (2014). <https://doi.org/10.1016/j.fuel.2014.02.038>
- 674 48. Arena, U., Di Gregorio, F.: Fluidized bed gasification of industrial solid recovered fuels. *Waste*
 675 *Manag.* 50, 86–92 (2016). <https://doi.org/10.1016/j.wasman.2016.02.011>
- 676 49. Wilk, V., Hofbauer, H.: Conversion of fuel nitrogen in a dual fluidized bed steam gasifier. *Fuel*.
 677 106, 793–801 (2013). <https://doi.org/10.1016/j.fuel.2012.12.056>
- 678 50. Berruoco, C., Recari, J., Abelló, S., Farriol, X., Montané, D.: Experimental Investigation of Solid
 679 Recovered Fuel (SRF) Gasification: Effect of Temperature and Equivalence Ratio on Process
 680 Performance and Release of Minor Contaminants. *Energy Fuels*. 29, 7419–7427 (2015).
 681 <https://doi.org/10.1021/acs.energyfuels.5b02032>

- 682 51. Berruenco, C., Recari, J., Güell, B.M., Alamo, G. del: Pressurized gasification of torrefied woody
683 biomass in a lab scale fluidized bed. *Energy*. 70, 68–78 (2014).
684 <https://doi.org/10.1016/j.energy.2014.03.087>
- 685 52. Gas analysis in gasification of biomass and waste - Guideline report Document 1. IEA Bioenergy
686 Task 33 (2018)
- 687 53. Aljbour, S.H., Kawamoto, K.: Bench-scale gasification of cedar wood – Part II: Effect of
688 Operational conditions on contaminant release. *Chemosphere*. 90, 1501–1507 (2013).
689 <https://doi.org/10.1016/j.chemosphere.2012.08.030>
- 690 54. Recari, J., Berruenco, C., Abelló, S., Montané, D., Farriol, X.: Gasification of two solid recovered
691 fuels (SRFs) in a lab-scale fluidized bed reactor: Influence of experimental conditions on
692 process performance and release of HCl, H₂S, HCN and NH₃. *Fuel Process. Technol.* 142, 107–
693 114 (2016). <https://doi.org/10.1016/j.fuproc.2015.10.006>
- 694 55. Arena, U., Zaccariello, L., Mastellone, M.L.: Fluidized bed gasification of waste-derived fuels.
695 *Waste Manag.* 30, 1212–1219 (2010). <https://doi.org/10.1016/j.wasman.2010.01.038>
- 696 56. Pels, J.R., Kapteijn, F., Moulijn, J.A., Zhu, Q., Thomas, K.M.: Evolution of nitrogen functionalities
697 in carbonaceous materials during pyrolysis. *Carbon*. 33, 1641–1653 (1995).
698 [https://doi.org/10.1016/0008-6223\(95\)00154-6](https://doi.org/10.1016/0008-6223(95)00154-6)
- 699 57. Leppälahti, J., Koljonen, T.: Nitrogen evolution from coal, peat and wood during gasification:
700 Literature review. *Fuel Process. Technol.* 43, 1–45 (1995). [https://doi.org/10.1016/0378-3820\(94\)00123-B](https://doi.org/10.1016/0378-3820(94)00123-B)
- 702 58. Leppälahti, J., Kurkela, E.: Behaviour of nitrogen compounds and tars in fluidized bed air
703 gasification of peat. *Fuel*. 70, 491–497 (1991). [https://doi.org/10.1016/0016-2361\(91\)90026-7](https://doi.org/10.1016/0016-2361(91)90026-7)
- 704 59. Hansson, K.-M., Samuelsson, J., Tullin, C., Åmand, L.-E.: Formation of HNCO, HCN, and NH₃
705 from the pyrolysis of bark and nitrogen-containing model compounds. *Combust. Flame*. 137,
706 265–277 (2004). <https://doi.org/10.1016/j.combustflame.2004.01.005>
- 707 60. Kelemen, S.R., Afeworki, M., Gorbaty, M.L., Kwiatek, P.J., Sansone, M., Walters, C.C., Cohen,
708 A.D.: Thermal Transformations of Nitrogen and Sulfur Forms in Peat Related to Coalification.
709 *Energy Fuels*. 20, 635–652 (2006). <https://doi.org/10.1021/ef050307p>
- 710 61. Leichtnam, J., Schwartz, D., Gadiou, R.: The behaviour of fuel-nitrogen during fast pyrolysis of
711 polyamide at high temperature. *J. Anal. Appl. Pyrolysis*. 55, 255 (2000)
- 712 62. Scott, D.S., Piskorz, J.: The continuous flash pyrolysis of biomass. *Can. J. Chem. Eng.* 62, 404–
713 412 (1984). <https://doi.org/10.1002/cjce.5450620319>
- 714 63. Scott, D.S., Piskorz, J., Westerberg, I.B., McKeough, P.: Flash pyrolysis of peat in a fluidized bed.
715 *Fuel Process. Technol.* 18, 81–95 (1988). [https://doi.org/10.1016/0378-3820\(88\)90076-8](https://doi.org/10.1016/0378-3820(88)90076-8)
- 716 64. Tian, F.-J., Yu, J., McKenzie, L.J., Hayashi, J., Li, C.-Z.: Conversion of Fuel-N into HCN and NH₃
717 During the Pyrolysis and Gasification in Steam: A Comparative Study of Coal and Biomass.
718 *Energy Fuels*. 21, 517–521 (2007). <https://doi.org/10.1021/ef060415r>
- 719 65. Kurkela, E., Laatikainen, J., Ståhlberg, P.: Pressurized Fluidized-bed Gasification Experiments
720 with Wood, Peat and Coal at VTT in 1991-1992: Gasification of danish wheat straw and coal.
721 VTT (1996)
- 722 66. Glarborg, P., Jensen, A.D., Johnsson, J.E.: Fuel nitrogen conversion in solid fuel fired systems.
723 *Prog. Energy Combust. Sci.* 29, 89–113 (2003). [https://doi.org/10.1016/S0360-1285\(02\)00031-X](https://doi.org/10.1016/S0360-1285(02)00031-X)
- 724 X
- 725 67. Ma, W., Hoffmann, G., Schirmer, M., Chen, G., Rotter, V.S.: Chlorine characterization and
726 thermal behavior in MSW and RDF. *J. Hazard. Mater.* 178, 489–498 (2010).
727 <https://doi.org/10.1016/j.jhazmat.2010.01.108>
- 728 68. Bläsing, M., Zini, M., Müller, M.: Influence of Feedstock on the Release of Potassium, Sodium,
729 Chlorine, Sulfur, and Phosphorus Species during Gasification of Wood and Biomass Shells.
730 *Energy Fuels*. 27, 1439–1445 (2013). <https://doi.org/10.1021/ef302093r>

- 731 69. Corella, J., Toledo, J.M., Molina, G.: Performance of CaO and MgO for the hot gas clean up in
732 gasification of a chlorine-containing (RDF) feedstock. *Bioresour. Technol.* 99, 7539–7544
733 (2008). <https://doi.org/10.1016/j.biortech.2008.02.018>
- 734 70. Lu, H., Purushothama, S., Hyatt, J., Pan, W.-P., Riley, J.T., Lloyd, W.G., Flynn, J., Gill, P.: Co-firing
735 high-sulfur coals with refuse-derived fuel. *Thermochim. Acta.* 284, 161–177 (1996).
736 [https://doi.org/10.1016/0040-6031\(96\)02864-X](https://doi.org/10.1016/0040-6031(96)02864-X)
- 737 71. Jazbec, M., Sendt, K., Haynes, B.S.: Kinetic and thermodynamic analysis of the fate of sulphur
738 compounds in gasification products. *Fuel.* 83, 2133–2138 (2004).
739 <https://doi.org/10.1016/j.fuel.2004.06.017>
- 740 72. Tchapda, A., Pisupati, S., Tchapda, A.H., Pisupati, S.V.: A Review of Thermal Co-Conversion of
741 Coal and Biomass/Waste. *Energies.* 7, 1098–1148 (2014). <https://doi.org/10.3390/en7031098>
- 742 73. Knudsen, J.N., Jensen, P.A., Lin, W., Frandsen, F.J., Dam-Johansen, K.: Sulfur Transformations
743 during Thermal Conversion of Herbaceous Biomass. *Energy Fuels.* 18, 810–819 (2004).
744 <https://doi.org/10.1021/ef034085b>
- 745 74. Hervy, M., Pham Minh, D., Gérente, C., Weiss-Hortala, E., Nzihou, A., Villot, A., Le Coq, L.: H₂S
746 removal from syngas using wastes pyrolysis chars. *Chem. Eng. J.* 334, 2179–2189 (2018).
747 <https://doi.org/10.1016/j.cej.2017.11.162>
- 748 75. Broer, K.M., Brown, R.C.: The role of char and tar in determining the gas-phase partitioning of
749 nitrogen during biomass gasification. *Appl. Energy.* 158, 474–483 (2015).
750 <https://doi.org/10.1016/j.apenergy.2015.08.100>
- 751 76. Pinto, F., Lopes, H., André, R.N., Gulyurtlu, I., Cabrita, I.: Effect of catalysts in the quality of
752 syngas and by-products obtained by co-gasification of coal and wastes. 1. Tars and nitrogen
753 compounds abatement. *Fuel.* 86, 2052–2063 (2007).
754 <https://doi.org/10.1016/j.fuel.2007.01.019>
- 755 77. de Almeida, V.F., Gómez-Barea, A., Arroyo-Caire, J., Pardo, I.: On the Measurement of the Main
756 Inorganic Contaminants Derived from Cl, S and N in Simulated Waste-Derived Syngas. *Waste*
757 *Biomass Valorization.* (2020). <https://doi.org/10.1007/s12649-019-00879-4>
- 758 78. Hervy, M., Remy, D., Dufour, A., Mauviel, G.: Air-blown gasification of Solid Recovered Fuels
759 (SRFs) in lab-scale bubbling fluidized-bed-Influence of the operating conditions and of the SRF
760 composition. *Energy Convers. Manag.* 181, 584–592
- 761 79. Cluet, B., Mauviel, G., Rogaume, Y., Authier, O., Delebarre, A.: Segregation of wood particles in
762 a bubbling fluidized bed. *Fuel Process. Technol.* 133, 80–88 (2015).
763 <https://doi.org/10.1016/j.fuproc.2014.12.045>
- 764 80. Blanco, P.H., Wu, C., Onwudili, J.A., Williams, P.T.: Characterization of Tar from the
765 Pyrolysis/Gasification of Refuse Derived Fuel: Influence of Process Parameters and Catalysis.
766 *Energy Fuels.* 26, 2107–2115 (2012). <https://doi.org/10.1021/ef300031j>
- 767 81. Morin, M., Nitsch, X., Hémati, M.: Interactions between char and tar during the steam
768 gasification in a fluidized bed reactor. *Fuel.* 224, 600–609 (2018).
769 <https://doi.org/10.1016/j.fuel.2018.03.050>
- 770 82. Dufour, A., Masson, E., Girods, P., Rogaume, Y., Zoulalian, A.: Evolution of Aromatic Tar
771 Composition in Relation to Methane and Ethylene from Biomass Pyrolysis-Gasification. *Energy*
772 *Fuels.* 25, 4182–4189 (2011). <https://doi.org/10.1021/ef200846g>
- 773 83. Dufour, A., Girods, P., Masson, E., Rogaume, Y., Zoulalian, A.: Synthesis gas production by
774 biomass pyrolysis: Effect of reactor temperature on product distribution. *Int. J. Hydrog. Energy.*
775 34, 1726–1734 (2009). <https://doi.org/10.1016/j.ijhydene.2008.11.075>
- 776 84. Dufour, A., Valin, S., Castelli, P., Thiery, S., Boissonnet, G., Zoulalian, A., Glaude, P.-A.:
777 Mechanisms and Kinetics of Methane Thermal Conversion in a Syngas. *Ind. Eng. Chem. Res.* 48,
778 6564–6572 (2009). <https://doi.org/10.1021/ie900343b>
- 779 85. Jess, A.: Mechanisms and kinetics of thermal reactions of aromatic hydrocarbons from
780 pyrolysis of solid fuels. *Fuel.* 75, 1441–1448 (1996). [https://doi.org/10.1016/0016-](https://doi.org/10.1016/0016-2361(96)00136-6)
781 [2361\(96\)00136-6](https://doi.org/10.1016/0016-2361(96)00136-6)

- 782 86. Phan, T.S., Sane, A.R., Rêgo de Vasconcelos, B., Nzihou, A., Sharrock, P., Grouset, D., Pham
783 Minh, D.: Hydroxyapatite supported bimetallic cobalt and nickel catalysts for syngas production
784 from dry reforming of methane. *Appl. Catal. B Environ.* 224, 310–321 (2018).
785 <https://doi.org/10.1016/j.apcatb.2017.10.063>
- 786 87. Dupont, C., Jacob, S., Marrakchy, K.O., Hognon, C., Grateau, M., Labalette, F., Da Silva Perez,
787 D.: How inorganic elements of biomass influence char steam gasification kinetics. *Energy*. 109,
788 430–435 (2016). <https://doi.org/10.1016/j.energy.2016.04.094>
- 789 88. Bates, R.B., Altantzis, C., Ghoniem, A.F.: Modeling of Biomass Char Gasification, Combustion,
790 and Attrition Kinetics in Fluidized Beds. *Energy Fuels*. 30, 360–376 (2016).
791 <https://doi.org/10.1021/acs.energyfuels.5b02120>
- 792 89. Westbrook, C.K., Dryer, F.L.: Chemical kinetic modeling of hydrocarbon combustion. *Prog.*
793 *Energy Combust. Sci.* 10, 1–57 (1984). [https://doi.org/10.1016/0360-1285\(84\)90118-7](https://doi.org/10.1016/0360-1285(84)90118-7)
- 794 90. Battin-Leclerc, F.: Detailed chemical kinetic models for the low-temperature combustion of
795 hydrocarbons with application to gasoline and diesel fuel surrogates. *Prog. Energy Combust.*
796 *Sci.* 34, 440–498 (2008). <https://doi.org/10.1016/j.peccs.2007.10.002>
- 797 91. Debono, O., Villot, A.: Nitrogen products and reaction pathway of nitrogen compounds during
798 the pyrolysis of various organic wastes. *J. Anal. Appl. Pyrolysis*. 114, 222–234 (2015).
799 <https://doi.org/10.1016/j.jaap.2015.06.002>
- 800 92. Chen, H., Wang, Y., Xu, G., Yoshikawa, K.: Fuel-N Evolution during the Pyrolysis of Industrial
801 Biomass Wastes with High Nitrogen Content. *Energies*. 5, 5418–5438 (2012).
802 <https://doi.org/10.3390/en5125418>
- 803 93. Recari, J., Berruero, C., Abelló, S., Montané, D., Farriol, X.: Effect of Bed Material on
804 Oxygen/Steam Gasification of Two Solid Recovered Fuels (SRFs) in a Bench-Scale Fluidized-Bed
805 Reactor. *Energy Fuels*. 31, 8445–8453 (2017).
806 <https://doi.org/10.1021/acs.energyfuels.7b01507>
- 807 94. Ephraïm, A., Ngo, L., Pham Minh, D., Lebonnois, D., Peregrina, C., Sharrock, P., Nzihou, A.:
808 Valorization of Waste-Derived Inorganic Sorbents for the Removal of HCl in Syngas. *Waste*
809 *Biomass Valorization*. (2018). <https://doi.org/10.1007/s12649-018-0355-1>
- 810 95. Delgado, J., Aznar, M.P., Corella, J.: Biomass Gasification with Steam in Fluidized Bed:
811 Effectiveness of CaO, MgO, and CaO–MgO for Hot Raw Gas Cleaning. *Ind. Eng. Chem. Res.* 36,
812 1535–1543 (1997). <https://doi.org/10.1021/ie960273w>
- 813